Journal of Sound and Vibration 325 (2009) 755–768

Contents lists available at ScienceDirect

Journal of Sound and Vibration

journal homepage: www.elsevier.com/locate/jsvi

# Damage detection in composite structures using vibration response under stochastic excitation

Zhichun Yang *, Le Wang, Hui Wang, Yan Ding, Xiaojuan Dang

*School of Aeronautics, Northwestern Polytechnical University, Xi'an 710072, China*

ARTICLE INFO

*Article history:*
Received 10 July 2008
Received in revised form
20 January 2009
Accepted 27 March 2009
Handling Editor: L.G. Tham
Available online 5 May 2009

ABSTRACT

The investigations in damage detection methods based on vibration response are reviewed according to two categories, i.e. model-based damage detection method (MBDDM) and non-model-based damage detection method (NMBDDM). Then a new concept of inner product vector (IPV) is introduced using the cross correlation function of the measured vibration responses of the structure, and the corresponding damage detection method is proposed based on this vector. It is theoretically proved that the elements in IPV of a structure is the inner product of the time domain vibration responses of corresponding measurement points, and this vector can be directly calculated using the measured time domain vibration responses. Under white noise excitation the IPV of a structure is a weighted summation of mode shapes of the structure, and the weighted factors of the summation only depend on modal parameters of the structure. The effect of measurement noise on IPV is also considered, and the effect can be eliminated by the definition of IPV and an interpolation technique. The difference of IPVs between the intact and damaged structure is adopted as the damage index, and damage location is determined by the abrupt change in the difference of IPV. In order to distinguish the abrupt change caused by structural damage and measurement noise, two thresholds are proposed to classify the damaged and intact structures. Numerical simulation results of damage detection of single-location and multi-location delamination in a composite laminate beam demonstrate the effectiveness and veracity of the proposed method, even though measurement noise is considered in the vibration responses.



## 1. Introduction

Damage detection methods based on vibration tests are the hot topics that have received considerable attention in the literature in last three decades [1–3]. Local damage in the structure induce changes in local physical parameters (such as mass and stiffness) of the structure. These local physical parameters influence the modal parameters (such as natural frequencies, damping and mode shapes), as well as the vibration responses of the structure. Therefore, changes in modal parameters or vibration responses can be utilized in vibration-based damage detection method to identify changes in physical parameters of the structure. On the other hand, most engineering structures are subjected to ambient dynamic loads and/or working dynamic loads, and the vibration response signals can be measured easily by conventional dynamic testing technique. It is clear that damage detection methods based on vibration can be performed as a real-time or online

* Corresponding author. Tel./fax: +86 29 88460461.
*E-mail addresses:* yangzc@nwpu.edu.cn (Z.C. Yang), wanglnpu@126.com, wangle@mail.nwpu.edu.cn (L. Wang).

0022-460X/$ - see front matter 
doi:10.1016/j.jsv.2009.03.040

**Nomenclature**

| | |
|---|---|
| $A_{ijk}^r$ | coefficient dependent on the $r$th modal parameters, response points $i$, $j$, and excitation point $k$ |
| $B_{ijk}^r$ | coefficient dependent on the $r$th modal parameters, response points $i$, $j$, and excitation point $k$ |
| $\mathbf{D}_{\mathrm{IPV}}$ | change in normalized IPVs between the intact and damaged structures |
| $\mathbf{D}''_{\mathrm{IPV}}$ | second-order difference of $\mathbf{D}_{\mathrm{IPV}}$ |
| $I_{rs}$ | coefficient dependent on the $r$th and $s$th modes |
| $J_{rs}$ | coefficient dependent on the $r$th and $s$th modes |
| $m^r$ | $r$th modal mass |
| $n$ | number of modes |
| $N$ | length of discrete stochastic process |
| $N_m$ | $N_{IPV}-1$ |
| $N_{IPV}$ | number of elements in IPV |
| $R_{xy}$ | cross correlation function of $x$, $y$ |
| $\hat{R}_{xy}$ | unbiased estimate value of the cross correlation function |
| $R_{ijk}$ | cross correlation function of displacement responses |
| $R_{\mathrm{IPV}}$ | normalized inner product vector |
| $\hat{R}_{\mathrm{IPV}}$ | inner product vector directly calculated by inner product of the responses |
| $R_{\mathrm{IPV},i}$ | $i$th element of IPV without measurement noise |
| $R_{\mathrm{IPV},i}^m$ | $i$th element of IPV with measurement noise |
| $\mathbf{R}_{\mathrm{IPV}}^{\mathrm{damage}}$ | normalized IPV of the damaged structure |
| $\mathbf{R}_{\mathrm{IPV}}^{\mathrm{intact}}$ | normalized IPV of the intact structure |
| $T$ | time lag |
| $x$ | stochastic process |
| $\mathbf{x}_i$ | vibration response at point $i$ without measurement noise |
| $\mathbf{x}_j$ | vibration response at point $j$ without measurement noise |
| $\mathbf{x}_i^m$ | measured vibration response at point $i$ |
| $\mathbf{x}_j^m$ | measured vibration response at point $j$ |
| $y$ | stochastic process |
| $\alpha_k$ | coefficient depended on the statistical character of the white noise excitation. |
| $\beta_{jk}^{rs}$ | coefficient dependent on the $r$th and $s$th modal parameters, and reference response point $j$ and excitation point $k$ |
| $\gamma_{jk}^r$ | coefficient dependent on the modal parameters, and reference response point $j$ and excitation point $k$ |
| $\boldsymbol{\delta}_i$ | measurement noise on $\mathbf{x}_i^m$ |
| $\boldsymbol{\delta}_j$ | measurement noise on $\mathbf{x}_j^m$ |
| $\zeta^r$ | $r$th modal damping ratio |
| $\lambda$ | integral variable |
| $\sigma$ | standard deviation of normal distribution |
| $\phi_i^r$ | $i$th element in the $r$th mode shape |
| $\omega_d^r$ | $r$th damped natural frequency |
| $\omega_n^r$ | $r$th natural frequency |
| $E[\cdot]$ | expectation operator |
| $\mathrm{rms}(\cdot)$ | root mean square value operator |

*Subscript*

| | |
|---|---|
| $i$ | response measurement point |
| $j$ | reference response measurement point |
| $k$ | excitation point |

*Superscript*

| | |
|---|---|
| $r$ | $r$th mode |
| $s$ | $s$th mode |

damage detection method to overcome the drawbacks of the common nondestructive testing (NDT) techniques, such as acoustic emission, magnet fields, radiography, eddy-currents and thermal fields. These are usually offline method, and too expensive for extensive use in practice.

Depending upon whether an analytical model (which is usually FEM) of the structure is required, vibration-based damage detection methods can be classified as model-based damage detection methods (MBDDM) or non-model-based damage detection methods (NMBDDM).

In the MBDDM, the primary procedure is to build a precise analytical model of the intact structure by model updating techniques. At this rate, MBDDM can be further categorized into two types, the first type is referred to as model updating-based damage detection method (MUBDDM) in which both intact and damaged analytical model should be built precisely, while the second is called intact model-based damage detection method (IMBDDM) in which a precise analytical model of only the intact structure is required.

Many model updating methods can be performed as damage detection methods which are referred to as MUBDDM. Using natural frequencies and mode shapes, Fritzen and Bohle [4] compared the efficiency of four damage detection methods based on model updating, namely, the inverse eigen sensitivity method (IESM), the modal force residual method (MFRM), the pseudo-static method (PSM) and the minimization of the errors in the constitutive equations (MECE) approach. The damage detection for the STEELQUAKE benchmark showed that all the methods gave acceptable localization results. Görl and Link [5] utilized the difference between the test and analytical natural frequencies and mode shapes as the objective function of the model updating procedure. In their method, the reference FEM was updated by the modal parameters of the intact structure, while the FEM of the damaged structure was updated by the modal parameters of the damaged structure. Thus, the damage can be evaluated from the difference between the two FEM. The damage parameters of the COST benchmark steel frame were identified by this method. Based on the damage detection results of the Z24 bridge, Maeck and Roeck [6] concluded that the direct stiffness calculation using the natural frequencies and modal curvatures seems to be a good alternative for other detection methods like sensitivity-based updating techniques. Using the perturbation theory, a statistical damage identification algorithm based on natural frequency changes was developed by Xia and Hao [7] to account for the effects of random noise in both the vibration data and finite element model, and the feasibility of the proposed method was verified by Monte Carlo simulations. The effectiveness of the method was illuminated by the damage identification in a cantilever beam numerically and a cantilever plate experimentally. Hwang and Kim [8] proposed a model updating method by minimizing the difference between test and analytical FRFs. Only subsets of vectors from the full set of FRFs for a few frequencies were used in the model updating procedure. They then utilized the model updating procedure to identify the locations and severity of damage in structures. Simulation examples for a simple cantilever beam and a helicopter rotor blade demonstrated that the proposed method can identify the location and severity of damage in these structures precisely. Jaishi and Ren [9] proposed a sensitivity-based finite element model updating method for damage detection. The modal flexibility residual between the FEM and experiment model was adopted as the objective function. The damage detection results of a simulated example of the simply supported beam and a tested reinforced concrete beam demonstrated that the modal flexibility is sensitive to damage and the proposed damage detection method based on model updating is promising for the detection of damaged elements. Faverjon and Sinou [10] used the constitutive relation error (CRE) updating method [11–16] to update the intact and damaged structure respectively. Crack detection results of simulated beams demonstrated that the CRE updating method can detect the number of cracks on the beam and can estimate both the crack locations and sizes with satisfactory precision, even when 10% or 20% noise levels had been considered in the detection simulations.

The IMBDDM is another type of MBDDM which received considerable attentions. Similar to mode assurance criterion (MAC), Williams et al. [17] proposed the damage location assurance criterion (DLAC) which uses the frequency changes in a number of modes to identify the location of damage. In their method, the precise FEM was used to simulate a series of damage cases, and then the shift of natural frequencies between the damaged and intact structure were calculated, then the DLAC index was calculated using the natural frequencies of both the simulated damage in the FEM and the actual damage in the practice structure. Finally the maximum DLAC is used to locate the damage. Some numerical and experimental examples were used to verify the method and it was illustrated that the method can successfully detect a local stiffness change. Messina et al. [18] extend the DLAC to multiple damage location assurance criterion (MDLAC). The sensitivity analysis of natural frequency is used in the MDLAC method. The effectiveness of the method was illustrated using numerical data of two truss structures, and the damage detection result of a three-beam test structure showed that the proposed method provided good predictions of both the location and absolute size of damage at one or more sites. Shi et al. [19] proposed another MDLAC which utilized the mode shapes instead of natural frequencies in the MDLAC. In this method, the incomplete measured mode shapes are used to locate the damage, and then the natural frequencies are used to detect the damage position and extent again. It was shown that the mode shapes are more sensitive to damage location than natural frequencies. A numerical planar truss structure was used to verify that the new method is accurate and robust in damage localization with or without considering measurement noise.

Artificial neural networks (ANN) are widely used in the IMBDDM. The basic procedure of this method is to simulate a number of damage cases using a precise FEM of the intact structure at first; then, using the dynamic properties of the simulated damaged structures as the input and the damage states of the structures as the output, the ANN is trained. In the damage detection, the dynamic properties of the structure to be detected are used as the input of the trained ANN, and the output of the ANN is the damage state of the structure to be detected. Yam et al. [20] proposed an ANN and wavelet decomposition-based damage detection method. The input of the ANN is the energy spectrum variation of the structural vibration responses decomposed using wavelet package before and after the occurrence of damage. The effectiveness of the proposed method was illuminated by the crack damage detection for PVC sandwich plates. In order to reduce the computational task of the ANN-based damage detection method (which must simulate a number of damage cases), Yu et al. [21] introduced the advanced composite damage mechanics and the perturbation theory enhanced finite element method to the investigation of Yam et al. [20], and then the method was used to detect the crack of laminated composite shells partially filled with fluid [22,23].

Model updating, which must be used in MBDDM, is usually a complex task. Therefore, NMBDDM is introduced to improve the drawback of MBDDM. In the NMBDDM, the precise analytical model of the structure is not required, and the damage index is directly extracted from the dynamic responses or modal parameters. As the precise analytical model of the structure is not required, the advantage of NMBDDM is that the computation task is not so complex. Therefore, NMBDDM can be easily performed as real-time and online damage detection technique.

Generally speaking, there are two kinds of information adopted in NMBDDM, one is the modal parameters, and the other is vibration responses. As a number of damage information of the structure can be extracted from modal parameters, modal parameters are widely used in NMBDDM. Kim et al. [24] proposed two approaches to detect damage in structures for which a few natural frequencies or a few mode shapes are available. In the first approach, there are two algorithms, i.e. the damage-localization algorithm to locate damage from changes in natural frequencies, and the damage-sizing algorithm to estimate crack-size from natural frequency shift. In the second approach, a damage index algorithm to localize and estimate the severity of damage by monitoring changes in modal strain energy is formulated. Both of the two approaches are evaluated for several damage scenarios by locating and sizing damage in a numerically simulated prestressed concrete beams. For the sake of eliminating the erroneous assumptions in the existing mode shape-based methods, Choi and Park et al. [25] adopted additional modal information (natural frequencies) in the existing mode shape-based methods, and proposed a new damage index. The damage detection for a simulated simply supported plate showed that the proposed method yields superior damage quantification results over the existing algorithms. Alvandi and Cremona [26] reviewed four damage detection methods based on the change of natural frequencies and/or mode shapes, i.e. mode shape curvature method, flexibility change method, flexibility curvature change method and strain energy method. The probabilities of damage detection and the probabilities of false alarm were proposed in their investigation. The four damage detection methods were compared for a simple supported beam with different damage levels. Some important conclusions were obtained, such as the strain energy method presents the best stability regarding noisy signals.

Besides modal parameters, frequency response functions (FRF) of a structure also involve a lot of damage information of the structure. Park and Park [27] proposed a damage detection method based on incompletely measured frequency responses. They also discussed the frequency range in which the proposed method works efficiently. Both numerical and test examples showed that the proposed method can serve as an alternative to conventional damage detection methods.

As we know, the primary procedure of the damage detection methods based on modal parameters is modal analysis, and the damage detection methods based on FRFs need information on the external exciting force. Note that some of the modal parameters, such as mode shapes cannot be identified precisely, and it is difficult to identify the FRF of the structure under operation conditions. Therefore, the NMBDDMs, in which the vibration responses are used directly or indirectly, have also received considerable attention. Using the time domain vibration response of the structure, Worden et al. [28] proposed a damage detection method based on outlier analysis with the Mahalanobis squared distance. Damage detection results for four case studies (one simulation, two pseudo-experimental and one experimental) show that the method can identify the damage effectively. The same method was utilized by Sohn et al. [29] to distinguish data sets of a patrol boat of different structural conditions, and the detection results showed that the data sets can be clearly distinguished. Using the regression and interpolation approaches, the influence of the changing environment was considered by Worden et al. [30] in the damage detection based on outlier analysis, and a lumped mass system was utilized to illuminate the effectiveness of the method. Frequency domain signals, such as the transmissibility function which is defined as the ratio of Fourier transforms of the two responses at different locations of the structure, can also be used as damage index in NMBDDM. Worden [31] utilized the amplitude of the transmissibility function as the damage feature proxy vector. Then the auto-associative network (AAN) was trained using the damage feature as input and output, and the Euclidean distance between the input and output was used as damage index. The damage detection results of a simulated lumped-parameter mechanical system showed that the system transmissibility provides a sensitive feature for the detection of small stiffness changes. Using the transmissibility functions, outlier analysis, the capability of kernel density estimation and AAN were compared by Worden et al. [32], all the three methods can identify the present of damage in a laboratory metallic aircraft wing box, and the outlier analysis seems the easiest. Subsequently, they used the transmissibility function and outlier analysis to detect the presence of damage in a Gnat aircraft wing [33]. They then combined this technique with a multi-layer perceptron (MLP) network to detect the damage successfully, but the precondition of the damage localization is that the damage cases should be simulated on the Gnat aircraft [34].

Almost all of the NMBDDM mentioned above just can be performed to identify just the presence of the damage which is the lowest level of the four damage detection levels defined by Rytter [35]. How to use a NMBDDM to identify the damage location is a challenge. The authors of this paper have done some research in this area [36,37]. Using the cross correlation functions of the vibration responses under a steady random excitation with specific frequency spectrum, we proposed a damage detection approach based on the cross correlation function amplitude vector (CorV) in the former research. It was verified that under a steady random excitation with specific frequency spectrum, the CorV of a structure only depends on the frequency response function matrix of the structure, and it was also found that the normalized CorV has a specific shape. Thus the damage can be detected and located with the correlation and the relative difference between the CorVs obtained from intact and damaged structures. The results of some simulations and experimental examples demonstrated that the method can detect the presence and location of the damage correctly.

The damage detection method based on CorV verified that the cross correlation functions of the vibration responses under a steady random excitation are related with the modal parameters of the structure [36,37]. The modal analysis method called natural excitation technique (NExT), in which the response under random excitation are used to extract modal parameters, demonstrated that the cross correlation functions of the vibration responses under white noise excitation have the same form as the free response function (or impulse response function) [38,39]. Illuminated by these investigations, a new NMBDDM based on inner product vector (IPV) which is defined by the cross correlation function of the vibration responses under random excitation, is proposed in this paper.

## 2. Inner product vector

### 2.1. Background theory

The cross correlation function of two stochastic processes $x(t), y(t)$ is defined as

$$R_{xy}(T) = E[x(t+T)y(t)] \tag{1}$$

where $T$ is the time lag between the two stochastic process and $E[\cdot]$ the expectation of the stochastic variable.

Consider the two discrete stochastic processes $\mathbf{x} = [x_0, x_1, \ldots, x_{N-1}]^{\mathrm{T}}$ and $\mathbf{y} = [y_0, y_1, \ldots, y_{N-1}]^{\mathrm{T}}$, the unbiased estimate value of the cross correlation function is given by [40]

$$\hat{R}_{xy}(m) = \begin{cases} \dfrac{1}{N-m} \displaystyle\sum_{n=0}^{N-1-m} x_{n+m} y_n, & m \geqslant 0 \\ \hat{R}_{yx}(-m), & m < 0 \end{cases}, \quad -(N-1) \leqslant m \leqslant N-1 \tag{2}$$

When the time lag $T = 0$, the unbiased estimate of the cross correlation function is

$$\hat{R}_{xy}(0) = \frac{1}{N} \sum_{n=0}^{N-1} x_n y_n = \frac{1}{N} \langle \mathbf{x}, \mathbf{y} \rangle \tag{3}$$

where $\langle \mathbf{x}, \mathbf{y} \rangle$ is the inner product of the two vectors $\mathbf{x}$ and $\mathbf{y}$. From Eq. (3), we can deduce that, the value of the cross correlation function of two discrete stochastic processes at the time lag $T = 0$, is equal to the ratio of the inner product of the two discrete stochastic processes to the length of the discrete stochastic process.

### 2.2. Definition of IPV

Under white noise excitation (assuming that the excitation location is at point $k$), the cross correlation function of the displacement responses of the structure at point $i$ and $j$ is [38,39]

$$R_{ijk}(T) = \sum_{r=1}^{n} [A_{ijk}^r e^{-\zeta^r \omega_n^r T} \cos(\omega_d^r T) + B_{ijk}^r e^{-\zeta^r \omega_n^r T} \sin(\omega_d^r T)] \tag{4}$$

where $A_{ijk}^r$ and $B_{ijk}^r$ are independent of time lag $T$, are functions of only the modal parameters, and are shown below

$$\begin{Bmatrix} A_{ijk}^r \\ B_{ijk}^r \end{Bmatrix} = \sum_{s=1}^{n} \frac{\alpha_k \phi_i^r \phi_k^r \phi_j^s \phi_k^s}{m^r \omega_d^r m^s \omega_d^s} \int_0^{\infty} e^{(-\zeta^r \omega_n^r - \zeta^s \omega_n^s)\lambda} \sin(\omega_d^s \lambda) \begin{Bmatrix} \sin(\omega_d^r \lambda) \\ \cos(\omega_d^r \lambda) \end{Bmatrix} d\lambda \tag{5}$$

$A_{ijk}^r$ and $B_{ijk}^r$ can be further simplified by evaluating the integral

$$A_{ijk}^r = \sum_{s=1}^{n} \frac{\alpha_k \phi_i^r \phi_k^r \phi_j^s \phi_k^s}{m^r m^s \omega_d^r} \left[ \frac{I_{rs}}{J_{rs}^2 + I_{rs}^2} \right] \tag{6}$$

$$B_{ijk}^r = \sum_{s=1}^{n} \frac{\alpha_k \phi_i^r \phi_k^r \phi_j^s \phi_k^s}{m^r m^s \omega_d^r} \left[ \frac{J_{rs}}{J_{rs}^2 + I_{rs}^2} \right] \tag{7}$$

where

$$I_{rs} = 2\omega_d^r (\zeta^r \omega_n^r + \zeta^s \omega_n^s) \tag{8}$$

$$J_{rs} = (\omega_d^{s2} - \omega_d^{r2}) + (\zeta^r \omega_n^r + \zeta^s \omega_n^s)^2 \tag{9}$$

where $r = 1, 2, \ldots, n$ stands for $r$th modal parameter of the structure, $m^r$ is the $r$th modal mass, $\zeta^r$ the $r$th natural damping ratio, $\omega_n^r$ the $r$th natural frequency, $\omega_d^r$ the $r$th damped natural frequency, $\phi_i^r$ the $i$th element in the $r$th mode shape, $\alpha_k$ is a coefficient referred to the statistical character of the white noise excitation.

Therefore, under white noise excitation at point $k$, the value of the cross correlation function of the displacement responses at point $i_1$ (response measurement point) and point $j$ (reference response measurement point) at the time lag $T = 0$ is

$$R_{i_1jk}(0) = \alpha_k \sum_{r=1}^{n} \sum_{s=1}^{n} \frac{\phi_{i_1}^r \phi_k^r \phi_j^s \phi_k^s}{m^r m^s \omega_d^r} \left[ \frac{I_{rs}}{J_{rs}^2 + I_{rs}^2} \right] \tag{10}$$

Then, the $P$ dimensional vector can be defined as

$$\mathbf{R}_{\mathrm{IPV}} = [R_{i_1jk}(0), R_{i_2jk}(0), \ldots, R_{i_Pjk}(0)]^{\mathrm{T}} \tag{11}$$

$\mathbf{R}_{\mathrm{IPV}}$ is called the inner product vector, where the subscripts $i_1, i_2, \ldots, i_P$ indicate the response measurement points. Substituting Eq. (10) into Eq. (11), we obtain

$$\begin{aligned} \mathbf{R}_{\mathrm{IPV}} &= \alpha_k \sum_{r=1}^{n} \sum_{s=1}^{n} \frac{\phi_k^r \phi_j^s \phi_k^s}{m^r m^s \omega_d^r} \left[ \frac{I_{rs}}{J_{rs}^2 + I_{rs}^2} \right] [\phi_{i_1}^r, \phi_{i_2}^r, \ldots, \phi_{i_P}^r]^{\mathrm{T}} = \alpha_k \sum_{r=1}^{n} \sum_{s=1}^{n} \beta_{jk}^{rs} [\phi_{i_1}^r, \phi_{i_2}^r, \ldots, \phi_{i_P}^r]^{\mathrm{T}} \\ &= \alpha_k \sum_{r=1}^{n} \gamma_{jk}^r [\phi_{i_1}^r, \phi_{i_2}^r, \ldots, \phi_{i_P}^r]^{\mathrm{T}} = \alpha_k \sum_{r=1}^{n} \gamma_{jk}^r \boldsymbol{\varphi}^r \end{aligned} \tag{12}$$

where $\boldsymbol{\varphi}^r = [\phi^r_{i_1}, \phi^r_{i_2}, \ldots, \phi^r_{i_P}]^{\mathrm{T}}$ is the $r$th mode shape, $\beta^{rs}_{jk}$ is a coefficient which is dependent on the $r$th and $s$th modal parameters, and reference response position $j$ and excitation position $k$. Therefore, $\gamma^r_{jk}$ is a coefficient which is dependent on the modal parameters (including modal frequency, mode shape, modal damping ratio) and reference response position $j$ and excitation position $k$. $\mathbf{R}_{\mathrm{IPV}}$ is a combination of the mode shapes of the structure, and the contribution of each mode shape only depends on the modal parameters of the structure. Then we can predict that, the IPV of the structure can be utilized as a structural damage feature proxy vector.

It can be easily verified that the IPV can also be constructed using the velocity or the acceleration response, although all the equations above are deduced using the displacement response. Note that all the formulae used above are deduced based on the white noise excitation, but in practice, one can only simulate the white noise in a limited frequency range. As we know, provided that the power spectral density of the random signal is nearly a constant in the limited frequency range, the random excitation can be treated as white noise excitation. Therefore, the white noise with limited frequency range is adopted as the excitation in the following damage detection examples.

### 2.3. The effect of measurement noise on IPV

The measurement noise is unavoidable in vibration tests. In this section, firstly, the anti-noise ability of IPV is checked based on the assumption of Gaussian noise [32], then the anti-noise ability of IPV is extended to noise with an arbitrary distribution. Supposing the measured vibration responses of the measurement points $i$, $j$ are noted as $\mathbf{x}^m_i$ and $\mathbf{x}^m_j$ respectively, and $\mathbf{x}^m_i$ and $\mathbf{x}^m_j$ can be expressed as $\mathbf{x}^m_i = \mathbf{x}_i + \boldsymbol{\delta}_i$ and $\mathbf{x}^m_j = \mathbf{x}_j + \boldsymbol{\delta}_j$, where $\mathbf{x}_i$ and $\mathbf{x}_j$ are responses of the measurement points $i$, $j$ without measurement noise, respectively, $\boldsymbol{\delta}_i$ and $\boldsymbol{\delta}_j$ are the measurement noise on $\mathbf{x}^m_i$ and $\mathbf{x}^m_j$, respectively. The measurement noise, which is normally distributed with zero mean and standard deviation $\sigma$, is independent of the vibration response without measurement noise, i.e. $\delta_i \sim N(0, \sigma_i^2)$, $\delta_j \sim N(0, \sigma_j^2)$. The standard deviation $\sigma$ is depend on the noise level which will be defined in the following section. When $i \neq j$, the measurement noise $\delta_i$ is independent of $\delta_j$. Supposing the measurement point $j$ is the reference point, the element $R^m_{\mathrm{IPV},i}$ in the IPV, which is calculated from the vibration response of point $i$ and reference point $j$, can be expressed as

$$\begin{aligned} R^m_{\mathrm{IPV},i} &= R_{x^m_i x^m_j}(0) = E[x^m_i x^m_j] = E[(x_{i1} + \delta_{i1})(x_j + \delta_j)] = E[x_i x_j] + E[x_i \delta_j] + E[x_j \delta_i] + E[\delta_i \delta_j] \\ &= R_{\mathrm{IPV},i} + E[x_i]E[\delta_j] + E[x_j]E[\delta_i] + E[\delta_i \delta_j] = R_{\mathrm{IPV},i} + E[\delta_i \delta_j] \end{aligned} \tag{13}$$

where $R_{\mathrm{IPV},i}$ is the element of IPV which is calculated by the vibration response of the two measurement points without measurement noise. For different relationships of point $i$ and $j$, the following two cases should be considered:

When $i \neq j$, the measurement noise $\delta_i$ is independent of $\delta_j$, thus

$$R^m_{\mathrm{IPV},i} = R_{IPV,i} + E[\delta_i]E[\delta_j] = R_{\mathrm{IPV},i} \tag{14}$$

i.e. the IPV calculated by the measured responses with the supposed Gaussian noise is equal to the IPV calculated by the vibration responses without measurement noise, whilst the measurement point is different from the reference point.

When $i = j$, the measurement noise $\delta_i$ is equal to $\delta_j$. As $\delta_i \sim N(0, \sigma_i^2)$, thus, $\delta_i/\sigma_i \sim N(0,1)$, and $(\delta_i/\sigma_i)^2 \sim \chi^2(1)$, therefore, $E[\delta_i^2] = \sigma_i^2 E[(\delta_i/\sigma_i)^2] = \sigma_i^2$, then it gives

$$R^m_{\mathrm{IPV},i} = R_{\mathrm{IPV},i} + E[\delta_i^2] = R_{\mathrm{IPV},i} + \sigma_i^2 > R_{\mathrm{IPV},i} \tag{15}$$

i.e. the IPV calculated by the measured responses with the supposed Gaussian noise is larger than the IPV calculated by the vibration responses without measurement noise, whilst the measurement point is identical to the reference point.

As the element in the calculated IPV corresponding to the reference point (i.e. reference element) is seriously affected by the supposed Gaussian noise, it is inadequate to calculate it directly. To solve this problem, it is advised to calculate the value of reference element in IPV by interpolation using the elements in the vicinity of the reference point. In the following examples of this paper, the cubic spline is used for interpolation.

Using the same procedure as Eqs. (13)–(15), we can easily obtain the same conclusions, which were summarized for the supposed Gaussian noise, for the measurement noise satisfying the following three assumptions: (1) the measurement noise has an arbitrary distribution with zero mean; (2) the measurement noise is independent of the vibration responses without measurement noise and (3) the measurement noise of different measure positions are in dependent of each other.

### 2.4. The calculation of IPV

From Eqs. (3) and (11), the formula for calculating the IPV of the structure with these measurement points $i_1, i_2, \ldots, i_P$ and the reference measurement point $j$ is achieved as

$$\hat{\mathbf{R}}_{\mathrm{IPV}} = \frac{1}{N}[\langle \boldsymbol{x}_{i_1}, \boldsymbol{x}_j \rangle, \langle \boldsymbol{x}_{i_2}, \boldsymbol{x}_j \rangle, \ldots, \langle \boldsymbol{x}_{i_P}, \boldsymbol{x}_j \rangle]^{\mathrm{T}} \tag{16}$$

From Eq. (12), we know that there is a coefficient $\alpha_k$ related to the statistical character of the white noise excitation in IPV. Thus, in order to eliminate the influence of the magnitude of excitation force, the IPV should be normalized. In this paper, the IPV is normalized by its maximum value to make sure that the maximum value of the IPV is equal to unity

$$\mathbf{R}_{IPV} = \frac{\hat{\mathbf{R}}_{\mathrm{IPV}}}{\max(\hat{\mathbf{R}}_{\mathrm{IPV}})} \tag{17}$$

The IPV, which is a combination of the mode shapes, can be directly calculated by the vibration response in the time domain. Nevertheless, the modal identification procedure is not required in the calculation of the IPV. Therefore, the detection error, which may be induced by the modal identification in the damage detection method based on modal parameters, can be eliminated in the IPV-based damage detection method.

## 3. Damage localization based on the IPV

As we know, changes in local physical parameters will induce abrupt changes in local mode shapes. Accordingly, the IPV of the damaged structure will also have abrupt changes in the damage region. However, changes in physical parameters of the damage structure are usually rather small, so changes in IPV of the damaged structure will be smooth and cannot be distinguished clearly. Therefore, the damage index can be formulated using the difference between IPVs of the intact and damaged structures

$$\mathbf{D}_{\mathrm{IPV}} = \mathbf{R}_{\mathrm{IPV}}^{\mathrm{damage}} - \mathbf{R}_{\mathrm{IPV}}^{\mathrm{intact}} \tag{18}$$

where $\mathbf{R}_{\mathrm{IPV}}^{\mathrm{intact}}$ and $\mathbf{R}_{\mathrm{IPV}}^{\mathrm{damage}}$ are the IPV of the intact and damaged structure, respectively. In order to make changes in $\mathbf{D}_{\mathrm{IPV}}$ more clearly, the second-order difference of $\mathbf{D}_{\mathrm{IPV}}$ can be utilized to detect the abrupt changes

$$\mathbf{D}''_{\mathrm{IPV}}(i) = \mathbf{D}_{\mathrm{IPV}}(i+1) - 2\mathbf{D}_{\mathrm{IPV}}(i) + \mathbf{D}_{\mathrm{IPV}}(i-1) \tag{19}$$

where $i = 1, 2, \ldots, N_m - 1$, $N_m + 1$ is the number of the elements in $\mathbf{D}_{\mathrm{IPV}}$. The elements, which have the local maximum absolute value in $\mathbf{D}_{\mathrm{IPV}}$, is just the location(s) of the damage.

## 4. The simulation example of delamination localization in composite laminate beam

Composite laminates structures are widely utilized in structural engineering. Unfortunately they are apt to suffer delamination damage when they are subjected to low energy impact in service. As it is usually impossible to detect the delamination by visual inspection, the detection of the delamination damage becomes an important issue for these structures. In this section, the detection of delamination damage of a composite laminate beam is utilized as the simulation example to verify the feasibility and efficiency of the proposed damage detection method.

In order to simulate the structure's response to white noise excitation, the FEM model of the composite cantilever beam was built. As shown in Fig. 1, eight-node quadrilateral shell elements were used (25 in total) to model the $500\,\mathrm{mm} \times 40\,\mathrm{mm} \times 1.8\,\mathrm{mm}$ cantilever beam. An assistant study was performed to show that the 25 elements were not only enough for the calculation accuracy but also rapid for calculating the vibration responses of the beam. The stacking sequence of the intact beam is $[0°/45°/-45°/0°/90°/0°]_s$ and the thickness of the single layer is 0.15 mm [41]. The material is carbon fiber T300/QY8911 with density $\rho = 1610\,\mathrm{kg\,m^{-3}}$, elastic modulus $E_1 = 135\,\mathrm{GPa}$, $E_2 = 8.8\,\mathrm{GPa}$, shear modulus $G_{12} = 4.5\,\mathrm{GPa}$ and Poisson's ratio $\nu_{12} = 0.33$.

For the purpose of verifying the feasibility of the proposed method which can be used to locate the delamination correctly, three different delamination areas are simulated (see Fig. 1). The three delamination areas A1, A2 and A3 are the 6th element (which is 100 mm from the clamped edge), the 13th element (which is 240 mm from the clamped edge) and the 23rd element (which is 440 mm from the clamped edge) respectively. Based on these three simulated delamination damages, four damage cases (including three single-location delamination and one multi-location delamination) are simulated, as listed in Table 1. Damage case D1, D2 and D3, in which the delamination occurred on area A1, A2 and A3, respectively, are single-location delamination. Damage case D4, in which the delamination occurred on areas A1 and A2, is the multi-location delamination.

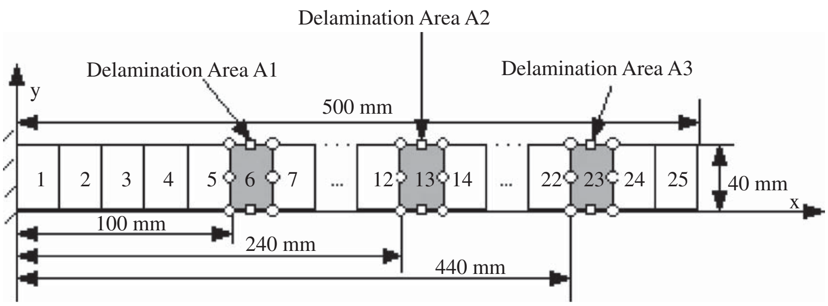


**Fig. 1.** The planform of the cantilevered laminate beam and its delamination locations.

Generally speaking, the delamination of the composite laminate structures always appears in the vicinity of its surface layers when the damage is induced by low energy impact load. Thus, it is assumed that the delamination occurred between the second and third layers, and the length of the delamination is 20 mm. The delamination of the composite beam is simulated as follows [42]: Firstly, the delaminated area element is copied; and then the upper and lower laminates are assigned the new stacking properties of [0°/45°] and [−45°/0°/90°/0°/0°/90°/−0°/−45°/45°/0°], respectively; finally the superposition nodes (the circled nodes in each damage case in Fig. 1) of both the intact and damage groups are merged together by constraining all of their dof.

The fundamental natural frequencies of the intact and damaged beams of the four damage cases are 8.198, 7.930, 8.132, 8.198 and 7.870 Hz, respectively. It is obvious that the shift of the fundamental natural frequency is very slight for different damage cases. Suppose that the beam is subject to a transverse random excitation with a frequency range from 0 to 10 Hz which just involves the fundamental natural frequency of the beam. The excitation signal (the length is 10 s with sample frequency of 1024 Hz) is identical for the intact and damaged structures. The excitation is exerted on the middle node of the element at the free end. Suppose that viscous damping is used and the damping ratio is 0.06 for both the intact and damaged structures. The acceleration responses are calculated using the direct integration method, and then the acceleration responses of the nodes on the symmetry axis are acquired. In order to verify that the proposed method can work well when the excitations for intact and damaged structures are similar in the frequency domain but different in the time domain, the response of the intact structure acquired between 3 and 6 s is used as the reference response, and the responses of the intact and damaged structures acquired between 7 and 10 s is used as the response of the unknown damage states in the following detection examples, respectively.

### 4.1. Damage detection without measurement noise

Utilizing the acceleration responses calculated by the FEM of the beam, and choosing the left node of the 20th element as the reference point (as there is no measurement noise in the calculated acceleration response in this case, any of the nodes can serve as the reference point), the normalized IPVs $\mathbf{R}_{\mathrm{IPV}}$ of the beam are calculated. The detection results are shown in Figs. 2–6, where $\mathbf{D}_{\mathrm{IPV}}$ and $|\mathbf{D}''_{\mathrm{IPV}}|$ represent the shift of the IPV between the intact and damaged structures, and the absolute value of the second-order difference of the shift of the IPV between the intact and damaged structures, respectively.

As shown in Fig. 2, although there is a little difference between the IPVs of the intact structure under different excitation (Fig. 2(c)), there is not any abrupt change in the shift of the $|\mathbf{D}''_{\mathrm{IPV}}|$ (Fig. 2(d)). Thus, we can conclude that there is not any

**Table 1**
Description of the four damage cases.

| Damage case | D1 | D2 | D3 | D4 |
|---|---|---|---|---|
| Delamination area(s) | A1 | A2 | A3 | A1 and A2 |

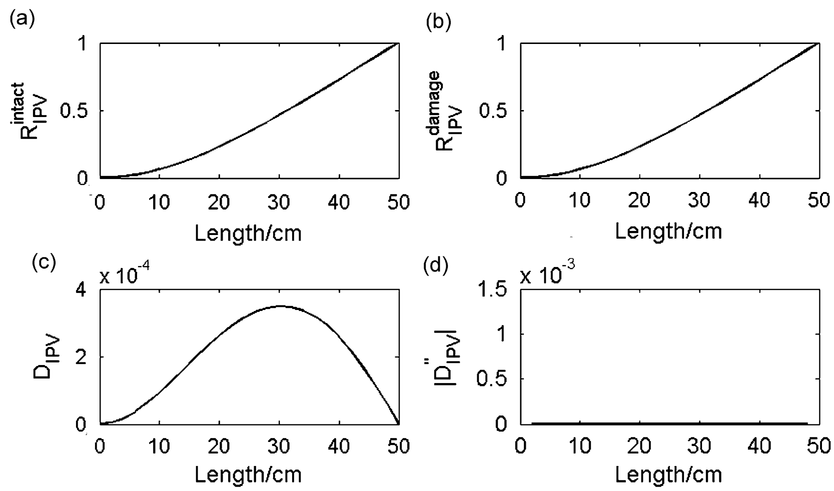


**Fig. 2.** Damage detection result of intact structure.

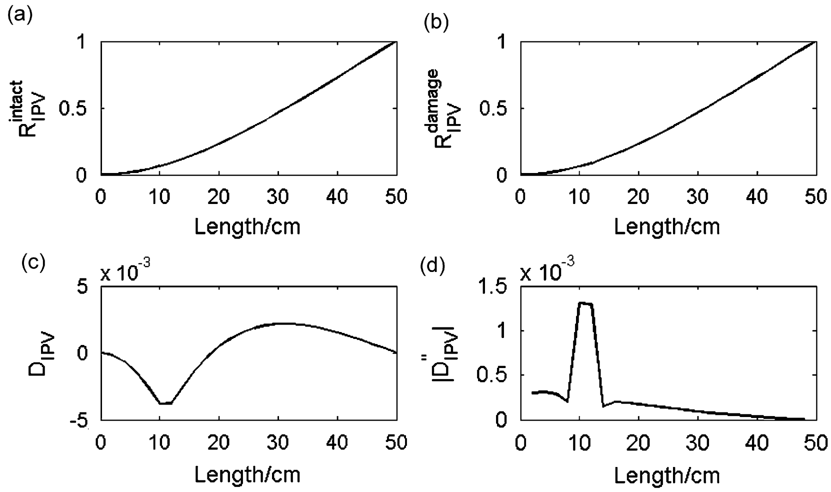


**Fig. 3.** Damage detection result of damage case D1.

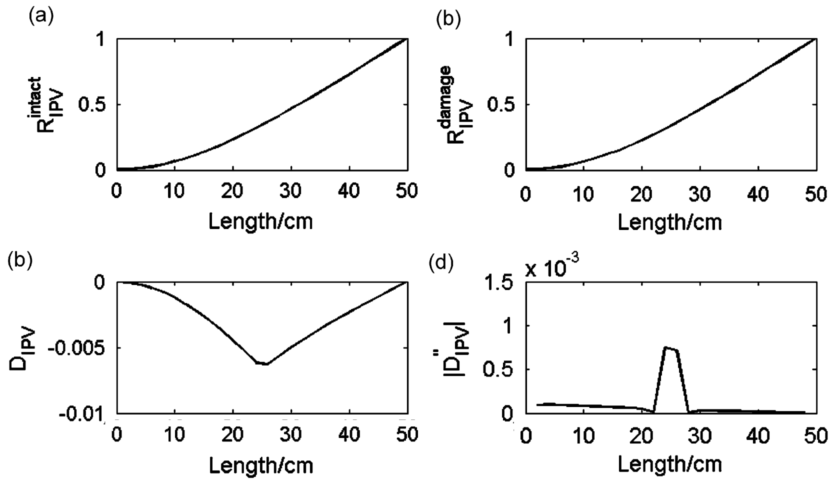


**Fig. 4.** Damage detection result of damage case D2.

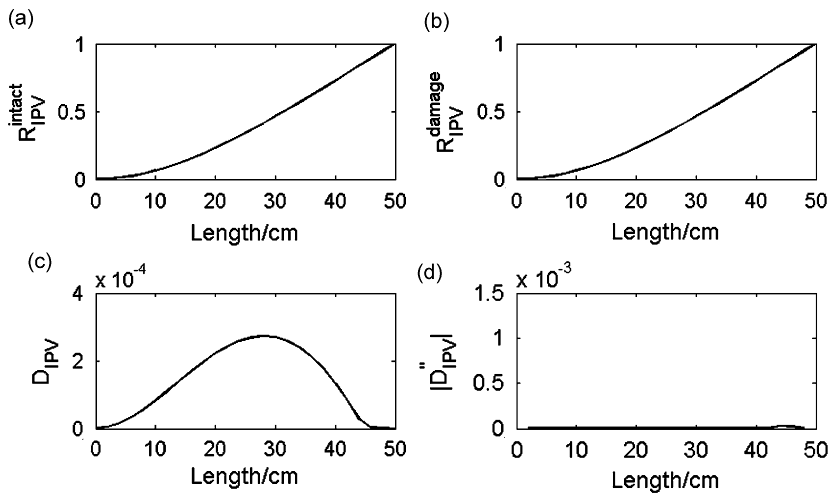


**Fig. 5.** Damage detection result of damage case D3.

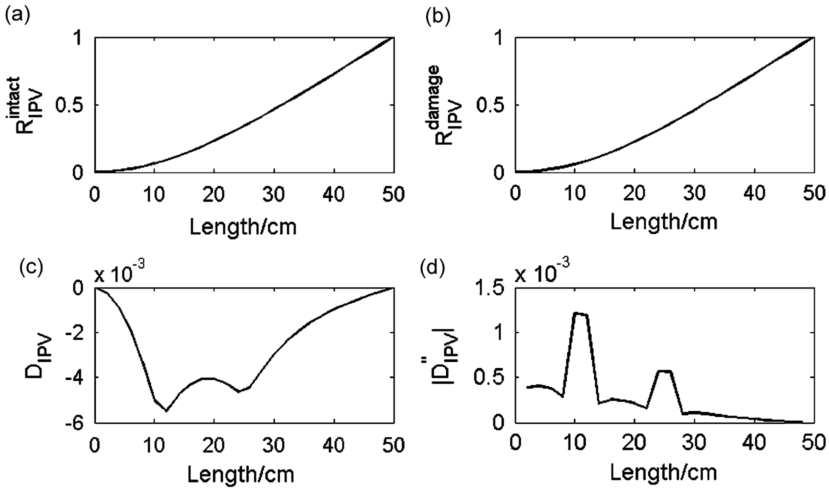


**Fig. 6.** Damage detection result of damage case D4.

damage in the beam. In Figs. 3 and 4, a distinct abrupt change occurred in $\mathbf{D}_{IPV}$ and $|\mathbf{D}''_{IPV}|$ (curves (c) and (d) in each figure), and the location of the abrupt change is just the simulated damage position. From Fig. 6, it can be seen that there are two distinct abrupt changes in $\mathbf{D}_{IPV}$ and $|\mathbf{D}''_{IPV}|$, and the locations of the two abrupt changes indicate the two simulated damage positions. Therefore, it can be concluded that the delamination(s) in the beam can be located by the abrupt change(s) in the $\mathbf{D}_{IPV}$ and $|\mathbf{D}''_{IPV}|$ curves correctly. Meanwhile, emphasis should be put on the discussion for the damage detection results of damage case D3 (Fig. 5). Although the damage can be identified from the $|\mathbf{D}''_{IPV}|$ curve in Fig. 5, the order of magnitude of $|\mathbf{D}''_{IPV}|$ in Fig. 5 is the same as that in Fig. 2, and less than that in Figs. 3, 4 and 6. This result illuminates that the damaged structure, in which the damage position is near the free end of the cantilever beam, cannot be detected clearly by the present method. It can be explained that the damage occurring near the free end has a very slight effect on the lower modal parameters. Therefore, the IPV calculated using the responses of the structure cannot obviously reflect the damage which is occurred near the free end of the cantilever beam.

### *4.2. Damage detection with measurement noise*

In Section 4.1, measurement noise is not considered. In this section measurement noise in the acceleration responses is considered to verify the robustness of the proposed method to noise. As mentioned in Section 2.3, it is supposed that the measurement noise is Gaussian noise with standard deviation $\sigma$ which depends on the noise level, and the measurement noise is independent of the value of the vibration response without measurement noise. The noise level is defined as

$$\eta = \frac{\mathrm{rms}(\delta)}{\mathrm{rms}(x)} \times 100\% \tag{20}$$

where rms(·) indicates the root mean square value of the signal, $x$ is the signal without measurement noise and $\delta$ is the added noise of $x$. In this paper, four different levels of measurement noise are considered for each acceleration response of the intact and damaged structures. The four measurement noise levels are 1%, 3%, 5% and 10%, respectively. For each noise level, 200 sets of simulation are performed, and the mean value of the IPVs of the 200 simulations is utilized to detect the damage.

In the damage detection with measurement noise, the threshold is introduced to detect and locate the damage of the structure. The position corresponding to the value of $|\mathbf{D}''_{IPV}|$, which is greater than the threshold, is identified as the damage location. As the threshold is related to many factors, such as the noise level of the measurement, the confidence level for the presence of damage, and so on, it is a rather difficult task to define an adequate threshold. Many damage detection methods are faced with the same problem of defining the threshold. In the damage detection method based on outlier analysis [28–34], the authors used Monte Carlo simulation to define a threshold which is just dependent on the number and dimension of the observation vectors. But the threshold of outlier analysis is only used to identify the present of the damage, except the case for damage localization when the outlier analysis is incorporated with ANN using plenty of experimental data [34]. The thresholds in some damage detection methods were defined by statistics, but numbers of data (simulated or experimental) of the intact and damaged structures were required in this procedure [26,43]. For the

IPV-based damage detection method, two different approaches to define the threshold are proposed. In the first approach, the threshold, named *invariable threshold*, is defined as a determined scalar based on a number of simulated or experimental results. In the second approach, the threshold, named *variable threshold*, is defined by the $3\sigma$ criterion based on the $|\mathbf{D}''_{\mathrm{IPV}}|$ curve, i.e. $I_{\mathrm{threshold}} = \mu_{|\mathbf{D}''_{\mathrm{IPV}}|} + 3\sigma_{|\mathbf{D}''_{\mathrm{IPV}}|}$ (where $I_{\mathrm{threshold}}$ is the threshold of $|\mathbf{D}''_{\mathrm{IPV}}|$, $\mu_{|\mathbf{D}''_{\mathrm{IPV}}|}, \sigma_{|\mathbf{D}''_{\mathrm{IPV}}|}$ stand for the mean value and stand deviation of $|\mathbf{D}''_{\mathrm{IPV}}|$).

Based on lots of simulations, the *invariable threshold* is selected as $0.5 \times 10^{-3}$ for all the damage cases of the cantilever beam, and the *variable threshold* is defined using the $3\sigma$ criterion. The damage detection results using both the *invariable threshold* and *variable threshold* are shown in Figs. 7–11, respectively.

As shown in Fig. 7, the $|\mathbf{D}''_{\mathrm{IPV}}|$ of the intact structure for all the noise levels are below both the *invariable threshold* and *variable threshold*, and it indicates that there no damage was occurred to the beam in this case. From Figs. 8 and 9, it can be

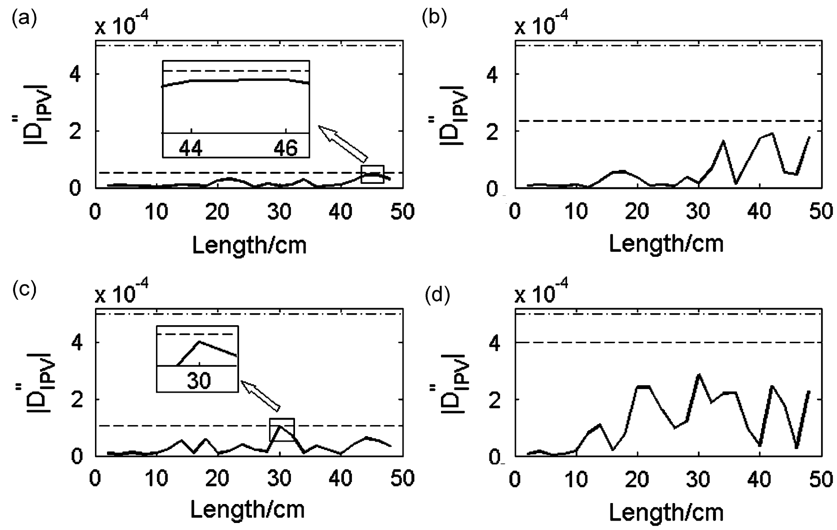


**Fig. 7.** Damage detection result of intact structure with measurement noise, (a), (b), (c) and (d) indicate that the noise level is 1%, 3%, 5% and 10%, respectively. – · – · *invariable threshold* and – – – *variable threshold*.

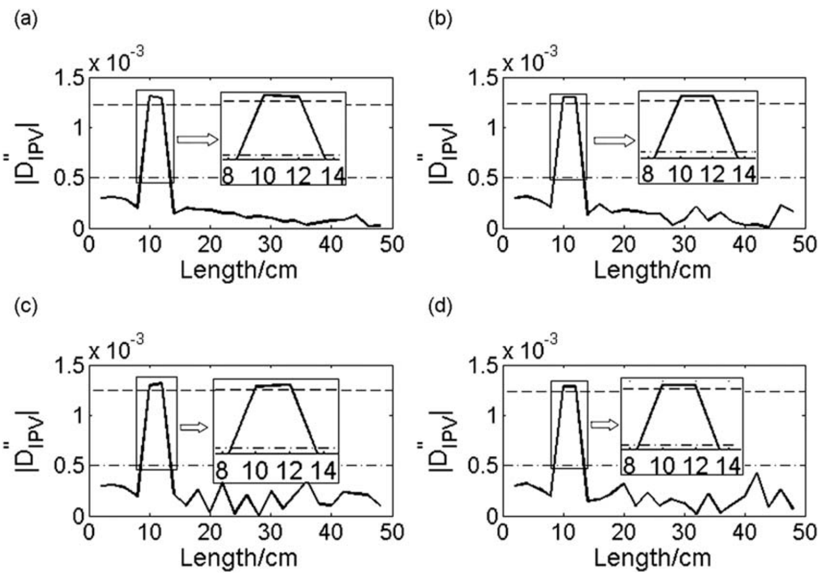


**Fig. 8.** Damage detection result of damage case D1 with measurement noise (a), (b), (c) and (d) indicate that the noise level is 1%, 3%, 5% and 10%, respectively. – · – · *invariable threshold* and – – – *variable threshold*.

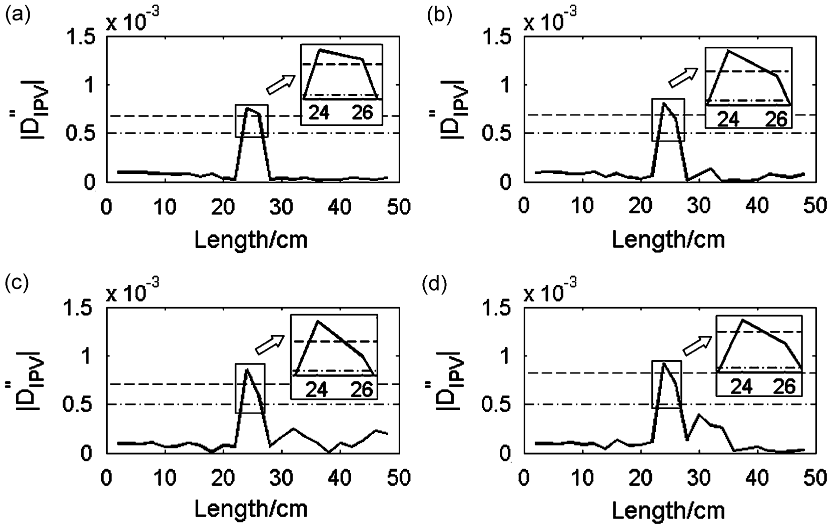


**Fig. 9.** Damage detection result of damage case D2 with measurement noise (a), (b), (c) and (d) indicate that the noise level is 1%, 3%, 5% and 10%, respectively. – · – · *invariable threshold* and – – – *variable threshold*.

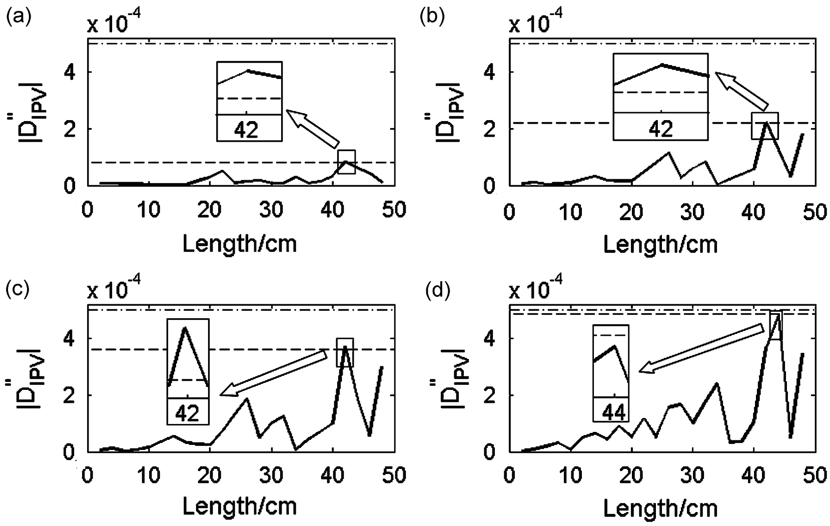


**Fig. 10.** Damage detection result of damage case D3 with measurement noise (a), (b), (c) and (d) indicate that the noise level is 1%, 3%, 5% and 10%, respectively. – · – · *invariable threshold* and – – – *variable threshold*.

seen that the delamination area is correctly identified by the proposed method using either the *invariable threshold* or *variable threshold*, even when 10% noise levels had been considered. It also shows that the effectiveness of the proposed method will decrease with the increase of the noise level. In Fig. 10, the $|\mathbf{D}''_{\mathrm{IPV}}|$ of damage case D3 for all the noise levels are below the *invariable threshold* which indicates that the proposed method cannot be used to localize the delamination near the free end of the cantilever beam when using the *invariable threshold* $0.5 \times 10^{-3}$; but the delamination area can be detected and located correctly when using the *variable threshold* except that a false negative occurred when the noise level was 10%. Fig. 11 shows that the delamination areas can be detected and located correctly when using the *invariable threshold* $0.5 \times 10^{-3}$, but a false negative occurred for all the noise levels when using the *variable threshold*.

From the results of damage detection with measurement noise, a helpful conclusion for how to choose an appropriate threshold can be can be summarized, i.e. when we use the minimum of the invariable threshold and variable threshold, the proposed method can be used to localize the single-delamination damage and the multi-delamination damages near the root and middle of the cantilever beam, even if the measurement noise up to 10% is considered.

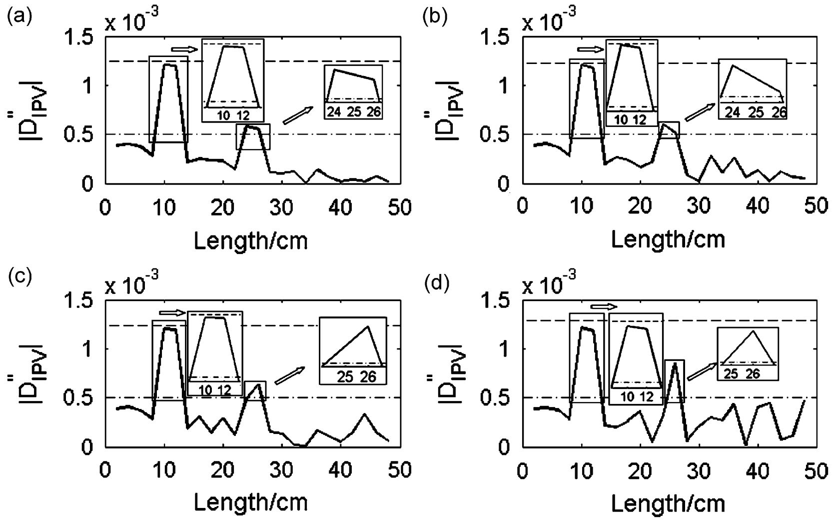


**Fig. 11.** Damage detection result of damage case D4 with measurement noise (a), (b), (c) and (d) indicate that the noise level is 1%, 3%, 5% and 10%, respectively. – · – · *invariable threshold* and – – – *variable threshold*.

## 5. Conclusions

The new concept of IPV is proposed in this paper, and it is proved that under white noise excitation the IPV of the structure is dependent on the modal parameters of the structure. Using the IPV as a damage index, the corresponding detection method is presented. The damage detection examples for the delamination damage of a composite beam show that

(1) The IPV-based damage detection method can locate the delamination of the composite beam correctly, even if the measurement noise of up to 10% of the root mean square value of the response signal is considered.
(2) In the IPV-based damage detection method, only the vibration responses excited by random excitation are required, and it is clear that in practice, the finite element model of the structure is not required. As the algorithm is rather simple, the IPV-based damage detection method can be used as a real-time or online damage detection method.

Nevertheless, like many of the existing damage detection methods, the IPV-based damage detection method cannot be used to locate the damage if the influence of the damage on the structures dynamics is too slight when the measurement noise is too large. Though almost all the damage cases were detected by the minimum of the invariable threshold and variable threshold, how to choose a more appropriate threshold for damage detection is a critical issue for such a method. Meanwhile, the other shortage of the IPV-based damage detection method is the cost of sensors which means that the sensor should be located close to the damage.

## Acknowledgements

This work was funded by the Project of New Century Excellent Talents in University of China (Grant no. NCET-04-0965), the Aeronautical Science Foundation of China (Grant no. 04I53072) and the Specialized Research Fund for the Doctoral Program of Higher Education of China (Grant no. 20060699001), the authors are also grateful to Dr Tim Waters and the reviewers for their kind help in revising the manuscript.

## References

[1] S.W. Doebling, C.R. Farrar, M.B. Prime, et al., Damage identification and health monitoring of structural and mechanical systems from changes in their vibration characteristics: a literature review, Los Alamos National Laboratory Report LA-13070-MS, 1996.
[2] H.S. Sohn, C.R. Farrar, F.M. Hemez, et al., A review of structural health monitoring literature: 1996–2001, Los Alamos National Laboratory Report LA-13976-MS, 2003.
[3] C.R. Farrar, K. Worden, An introduction to structural health monitoring, *Philosophical Transactions of the Royal Society A* 365 (2007) 303–305.
[4] C.-P. Fritzen, K. Bohle, Global damage identification of the 'STEELQUAKE' structure using modal data, *Mechanical Systems and Signal Processing* 17 (1) (2003) 111–117.
[5] E. Görl, M. Link, Damage identification using changes of eigen frequencies and mode shapes, *Mechanical Systems and Signal Processing* 17 (1) (2003) 103–110.
[6] J. Maeck, G.D. Roeck, Damage assessment using vibration analysis on the Z24-bridge, *Mechanical Systems and Signal Processing* 17 (1) (2003) 133–142.

[7] Y. Xia, H. Hao, Statistical damage identification of structures with frequency changes, *Journal of Sound and Vibration* 263 (2003) 853–870.
[8] H.Y. Hwang, C. Kim, Damage detection in structures using a few frequency response measurement, *Journal of Sound and Vibration* 270 (2004) 1–14.
[9] B. Jaishi, W. Ren, Damage detection by finite element model updating using modal flexibility residual, *Journal of Sound and Vibration* 292 (2006) 179–202.
[10] B. Faverjon, J.-J. Sinou, Robust damage assessment of multiple cracks based on the frequency response function and the constitutive relation error updating method, *Journal of Sound and Vibration* 312 (2008) 821–837.
[11] A. Deraemaeker, P. Ladeveze, S.Le. Loch, Result obtained by the CRE updating method using a plate model, *Mechanical Systems and Signal Processing* 17 (1) (2003) 47–54.
[12] J.Ph. Combe, P. Ladeveze, J.P. Pelle, Constitutive relation error estimator for transient finite element analysis, *Computer Methods in Applied Mechanics and Engineering* 176 (1999) 165–185.
[13] P. Ladeveze, A. Chouaki, Application of a posteriori error estimation for structural model updating, *Inverse Problems* 15 (1999) 49–58.
[14] A.T. Choudki, P. Ladeveze, L. Proslier, Updating structural dynamic models with emphasis on the damping properties, *AIAA Journal* 36 (6) (1998) 1094–1099.
[15] A. Deraemaeker, P. Ladeveze, Ph. Leconte, Reduced bases for model updating in structural dynamics based on constitutive relation error, *Computer Methods in Applied Mechanics and Engineering* 191 (2002) 2427–2444.
[16] D. Barthe, A. Deraemeaker, P. Ladeveze, et al., Validation and updating of industrial models based on the constitutive relation error, *AIAA Journal* 42 (7) (2004) 1427–1434.
[17] E.J. Williams, A. Messina, B.S. Payne, A frequency-change correlation approach to damage detection, *Proceedings of the 15th International Modal Analysis Conference* (*IMAC*), Orlando, FL, USA, 3–6 February 1997, pp. 652–657.
[18] A. Messina, E.J. Williams, T. Contursi, Structural damage detection by a sensitivity and statistical-based method, *Journal of Sound and Vibration* 216 (5) (1998) 791–808.
[19] Z.Y. Shi, S.S. Law, L.M. Zhang, Damage localization by directly using incomplete mode shapes, *Journal of Engineering Mechanics* 126 (6) (2000) 656–660.
[20] L.H. Yam, Y.J. Yan, J.S. Jiang, Vibration-based damage detection for composite structures using wavelet transform and neural network identification, *Composite Structures* 60 (2003) 403–412.
[21] L. Yu, L. Cheng, L.H. Yam, et al., Application of eigenvalue perturbation theory for detecting small structural damage using dynamic responses, *Composite Structures* 78 (2007) 402–409.
[22] L. Yu, L. Cheng, L.H. Yam, et al., Experimental validation of vibration-based damage detection for static laminated composite shells partially filled with fluid, *Composite Structures* 79 (2007) 288–299.
[23] L. Yu, L. Cheng, L.H. Yam, et al., Online damage detection for laminated composite shells partially filled with fluid, *Composite Structures* 80 (2007) 334–342.
[24] J.-T. Kim, Y.-S. Ryu, H.-M. Cha, et al., Damage identification in beam-type structures: frequency-based method vs mode-shape-based method, *Engineering Structures* 25 (2003) 57–67.
[25] S. Choi, S. Park, N.-H. Park, et al., Improved fault quantification for plate structure, *Journal of Sound and Vibration* 297 (2006) 865–879.
[26] A. Alvandi, C. Cremona, Assessment of vibration-based damage identification techniques, *Journal of Sound and Vibration* 292 (2006) 179–202.
[27] N.-G. Park, Y.-S. Park, Damage detection using spatially incomplete frequency response functions, *Mechanical Systems and Signal Processing* 17 (3) (2003) 519–532.
[28] K. Worden, G. Manson, N.R. Fieller, Damage detection using outlier analysis, *Journal of Sound and Vibration* 229 (3) (2000) 647–667.
[29] H. Sohn, C.R. Farrar, N.F. Hunter, et al., Structural health monitoring using statistical pattern recognition techniques, *Journal of Dynamic Systems, Measurement, and Control* 123 (12) (2001) 706–711.
[30] K. Worden, H. Sohn, C.R. Farrar, Novelty detection in a changing environment: regression and interpolation approaches, *Journal of Sound and Vibration* 258 (4) (2002) 741–761.
[31] K. Worden, Structural fault detection using a novelty measure, *Journal of Sound and Vibration* 201 (1) (1997) 85–101.
[32] K. Worden, G. Manson, D.J. Allman, Experimental validation of a structural health monitoring methodology—part I: novelty detection on a laboratory structure, *Journal of Sound and Vibration* 259 (2) (2003) 323–343.
[33] G. Manson, K. Worden, D.J. Allman, Experimental validation of a structural health monitoring methodology—part II: novelty detection on a Gnat aircraft, *Journal of Sound and Vibration* 259 (2) (2003) 344–364.
[34] G. Manson, K. Worden, D.J. Allman, Experimental validation of a structural health monitoring methodology—part III: damage location on a Gnat aircraft, *Journal of Sound and Vibration* 259 (2) (2003) 365–385.
[35] A. Rytter, Vibration-Based Inspection of Civil Engineering Structures, PhD Thesis, Department of Building Technology and Structural Engineering, University of Aalborg, Denmark, 1993.
[36] Z.F. Yu, Z.C. Yang, Damage detection based on the cross correlation function amplitude vector and its application to the ASCE benchmark structure, *Key Engineering Materials* 353–358 (2007) 2317–2320.
[37] Z.C Yang, Z.F. Yu, H. Sun, On the cross correlation function amplitude vector and its application to structural damage detection, *Mechanical Systems and Signal Processing* 21 (2007) 2918–2932.
[38] G.H. James III, T.G. Carne, J.P. Lauffer, The natural excitation technique (NExT) for modal parameter extraction from operating structures, *Modal Analysis: The International Journal of Analytical and Experimental Modal Analysis* 10 (4) (1995) 260–277.
[39] C.R. Farrar, G.H. James III, System identification from ambient vibration measurements on a bridge, *Journal of Sound and Vibration* 205 (1) (1997) 1–18.
[40] S.J. Orfanidis, *Optimum Signal Processing: An Introduction*, second ed., Prentice-Hall, Englewood Cliffs, NJ, 1996.
[41] B.S. Liu, C. Huang, *Patran Step by Step*, China WaterPower Press, 2003.
[42] S.S. Kessler, S.M. Spearing, M.J. Atalla, et al., Damage detection in composite materials using frequency response, *Composites Part B: Engineering* 33 (2002) 87–95.
[43] S. Choi, S. Park, N.-H. Park, et al., Improved fault quantification for plate structure, *Journal of Sound and Vibration* 297 (2006) 865–879.